Dynamic Rheological Studies of Hydrophobic Interactions in Injectable Collagen Biomaterials

JOEL ROSENBLATT,* BRIAN DEVEREUX,† and DONALD G. WALLACE‡

Collagen Corporation, 2500 Faber Place, Palo Alto, California 94303

SYNOPSIS

Injectable collagen is a concentrated dispersion of collagen fibers in aqueous solution that is used to correct dermal contour defects through intradermal injection. The effect of hydrophobic forces on the rheology of concentrated dispersions of collagen fibers was studied by dynamic rheological measurements over temperatures ranging from 283 to 308 K. The results are interpreted in terms of the associated relaxation time spectra and the theory of Kamphuis et al. for concentrated dispersions. Increases in fiber rigidity are seen from a progressive decrease in the slope of the linear log G' (or G'') vs. log ω data recorded for these dispersions as temperature is increased. A molecular interpretation of this result was obtained by treating collagen fibers as a liquid crystalline phase of rigid-rod collagen molecules that have phase-separated from aqueous solution. Hydrophobic forces affect the volume fraction of water that is present in the phase-separated fibers, which, in turn, affects the rigidity of the fibers. Distinct yielding behavior (in the nonlinear viscoelastic region) occurs at temperatures above 293 K and reflects a gel transition. Thermal gelation of collagen dispersions is proposed to proceed through hydrophobically driven mechanisms of increased fiber rigidity and enhanced interfiber attractive forces. © 1993 John Wiley & Sons, Inc.

INTRODUCTION

Highly purified, injectable collagen has been successfully used as a biocompatible implant in the correction of dermal contour defects for many years.[1,2] Injectable collagen is manufactured by solubilizing Type I collagen from cow hide and (following purification) reconstituting the soluble collagen into fibrils by precipitation at neutral pH. The purification of collagen has been described in detail elsewhere.[3] The thermodynamics and kinetics of precipitation of aqueous solutions of Type I collagen have been studied extensively.[4-6] Studies of the rheological properties of concentrated dispersions of reconstituted collagen fibers have not been extensive. Limited previous work includes creep compliance measurements on concentrated collagen dispersions[7] and extrusion-force measurements on cross-linked collagen suspensions.[8]

Type I collagen molecules (300 nm long × 1.5 nm diameter rigid rod, 300 kDalton protein[9]) self-assemble into phase-separated fibers at neutral pH and at temperatures between 288 and 310 K. *In vitro* collagen fibril assembly displays two different growth phases when studied by turbidity measurements.[10] The first is a lag phase in which an as-yet undefined nucleation or early assembly event occurs.[6] This is followed by a growth phase where striated fibers appear. The molecular architecture of these fibers has been studied by electron microscopy[11] and X-ray diffraction.[12] They possess a regular stagger of approximately $\frac{1}{4}$ of a rod length between each (rod) molecule and its axially aligned neighbor. Wallace and Thompson[3] quantitatively modeled the kinetics of fiber growth using a nucleation and growth model. A recent electron microscope study[13] suggested that reconstituted collagen fibers can organize into higher-order structures when precipitation occurs in an unstirred system.

* To whom correspondence should be addressed.

† Present address: Department of Chemical Engineering, University of California-Berkeley, Berkeley, CA 94720.

‡ Present address: Celtrix Pharmaceuticals Inc., 3055 Patrick Henry Dr., Santa Clara, CA 95052.

Journal of Applied Polymer Science, Vol. 50, 953–963 (1993)
 CCC 0021-8995/93/060953-11

The effect of hydrophobic interactions on the kinetics of fibril assembly has been extensively studied.[5,6,14] The data exhibit a strong decrease in the half-time for fibrillogenesis when temperature is increased above a threshold temperature. The amino acid sequence of Type I collagen is well characterized[15] and the rodlike molecule contains 224 hydrophobic amino acid side chains (including phenylalanine, valine, leucine, isoleucine, and methionine) that are capable of hydrophobically bonding with hydrophobic side chains on adjacent molecules when configured in fibers. The model of Wallace[16] predicts that hydrophobic interactions contribute much larger stabilization energies to collagen fibers than do electrostatic interactions. In this study, hydrophobic forces were varied (measurements performed at different temperatures) but electrostatic forces were held nearly constant (measurements performed on dispersions with the same ionic strengths) in order to define the effect of hydrophobic interactions on the mechanical properties of collagen fiber dispersions.

EXPERIMENTAL

Collagen was isolated from bovine hide by swelling in acid and pulverization followed by solubilization with porcine pepsin. The solubilized collagen was purified as previously described.[3] The pepsin digestion reportedly removes all the *N*-terminal extrahelical peptide and the distal end of the *C*-terminal peptide, but the rodlike triple helix is not degraded.[17] Fibrillar collagen was obtained by precipitating the purified collagen solution (approx. 3 mg/mL protein in 10 m*M* HCl) in 20 m*M* sodium phosphate (final pH 7.2) as described elsewhere.[18] The precipitated collagen was centrifuged 45 min at 15,000 g to form a dense pellet (97.1 mg/mL protein concn.). The pellet was then diluted to 26 mg/mL (protein) with a final concentration of 20 m*M* phosphate (pH 7.2) and 0.13*M* sodium chloride. Samples were allowed to equilibrate at a temperature of 277 K for 1 month.

Dynamic rheological measurements were performed on a Rheometrics fluids spectrometer (RFS model 8400) for all samples using a parallel plate geometry. The cone and plate geometry was not applicable to these dispersions as the largest fiber sizes (over 100 microns) exceed gap spacings at the tip of a cone and plate. Frequency response was measured in the linear viscoelastic spectrum over 3 decades of frequency (10^{-1} to 10^{2} rad/s) using 50 mm-diameter parallel plates. The frequency response measurements were performed with gap spacings of approximately 2 mm. Rheological spectra were found to be independent of gap spacing for gaps greater than 1 mm. The linear viscoelastic spectra were measured at a constant strain of 1%. This strain was determined to be well within the linear viscoelastic limit as identical spectra were recorded for strains of less than 1% (i.e., G' and G'' independent of strain). Measurements were performed at temperatures ranging from 283 to 308 K using a hydrated chamber so that the dispersion did not dry out. Temperature control was provided by a Brinkman RM20 water bath connected to the RFS environmental chamber attachment. Samples were loaded by radial squeeze flow of the dispersion between the plates. This induces an initial radial (r) fiber alignment. Dynamic measurements that were performed on samples that were presheared (initial angular, θ, alignment) gave slightly different spectra. All measurements reported here are for dispersions with a presumably initial radial fiber alignment. Samples were allowed at least 3–4 h relaxation time following loading and reaching the desired temperature prior to measurement. The time interval was arrived at from stress-relaxation measurements in which samples relaxed to their yield stress values following imposition of initial strain displacements of 100% after approximately 2 h. The incubation period was also checked by repeating rheological measurements (with longer incubation) to ensure that the spectra were invariant.

Nonlinear dynamic spectra were also measured in the parallel plate geometry. The recorded G' and G'' are for nominal strains at the outer edge (radial direction) of the platen. For any given angular deformation of the sample, the applied strain is a function of radial position in this geometry. Values of G' and G'' computed from measured torques on the platen are rigorous only when G' and G'' are independent of strain (linear viscoelastic region). Since the computation of G' and G'' in the parallel plate geometry assumes G' and G'' are independent of strain, the computed G' and G'' values in the nonlinear viscoelastic region become progressively more inaccurate as strains are increased beyond the linear viscoelastic limit. To circumvent this problem, measurements were attempted in a couette geometry (concentric cylinders); however, reliable data was difficult to obtain because the dispersions could not be uniformly loaded in this geometry. The nonlinear spectra were recorded in a humidified environment. Spectra of G' and G'' vs. strain were recorded at a frequency of 1 rad/s. The selection of this frequency will be discussed later.

RESULTS

Figure 1 displays the frequency response of G' in the linear viscoelastic region for the series of temperatures over which measurements were performed. Figure 2 presents the plots of G'' corresponding to those in Figure 1. The data are quite linear when plotted log G' or G'' vs. log frequency (ω). Parameters a' and n', defined by

$$G' = a'\omega^{n'} \tag{1}$$

were calculated by linear regression of log G' vs. log ω and the results are tabulated in Table I over the range of T. Similar linear-least-squares parameters, a'' and n'', defined by

$$G'' = a''\omega^{n''} \tag{2}$$

were calculated by linear regression of log G'' vs. log ω and the results are tabulated in Table II. This power-law behavior is expected and is in agreement with recent theories describing polymer gels.[19] Nonlinear rheological spectra of G' and G'' vs. strain (ω = 1 rad/s) measured in the parallel plate geometry (despite the previously discussed inaccuracies) are presented in Figures 3 and 4, respectively.

Relaxation-time spectra $[H(t)]$ over 3 decades of frequency were computed from the linearly viscoelastic G' data using a second-order approximation[20]:

$$H(t) = \{dG'/d\ln\omega - 0.5[d^2G'/d\ln\omega^2]\}_{1/\omega=(t/2)^{1/2}} \tag{3}$$

and from the linearly viscoelastic G'' data also using a second-order approximation[20]:

$$H(t) = (2/\pi)[G'' - d^2G''/d\ln\omega^2]_{1/\omega=t} \tag{4}$$

By computing derivatives based on (1) and (2), the respective functions for $H(t)$ become

$$H(t) = [a'n'(1 - n'/2)2^{n'/2}]t^{-n'} \tag{5}$$

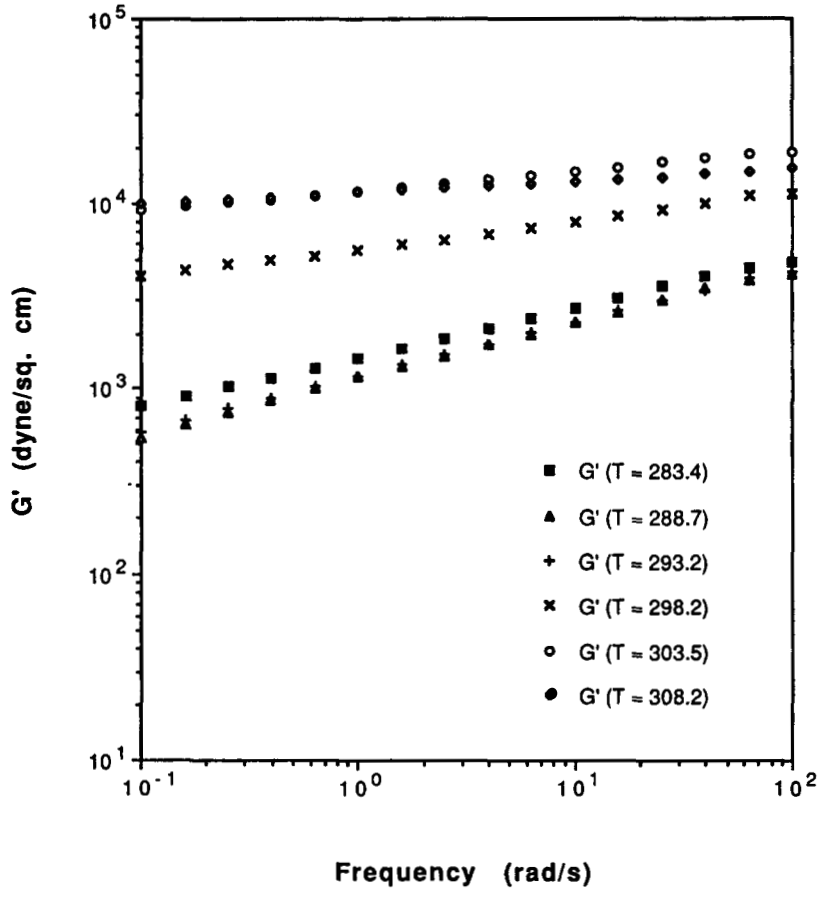

Figure 1 Dynamic rheological measurements in the linear viscoelastic region for G' vs. frequency. Measurement conditions are described in the text.

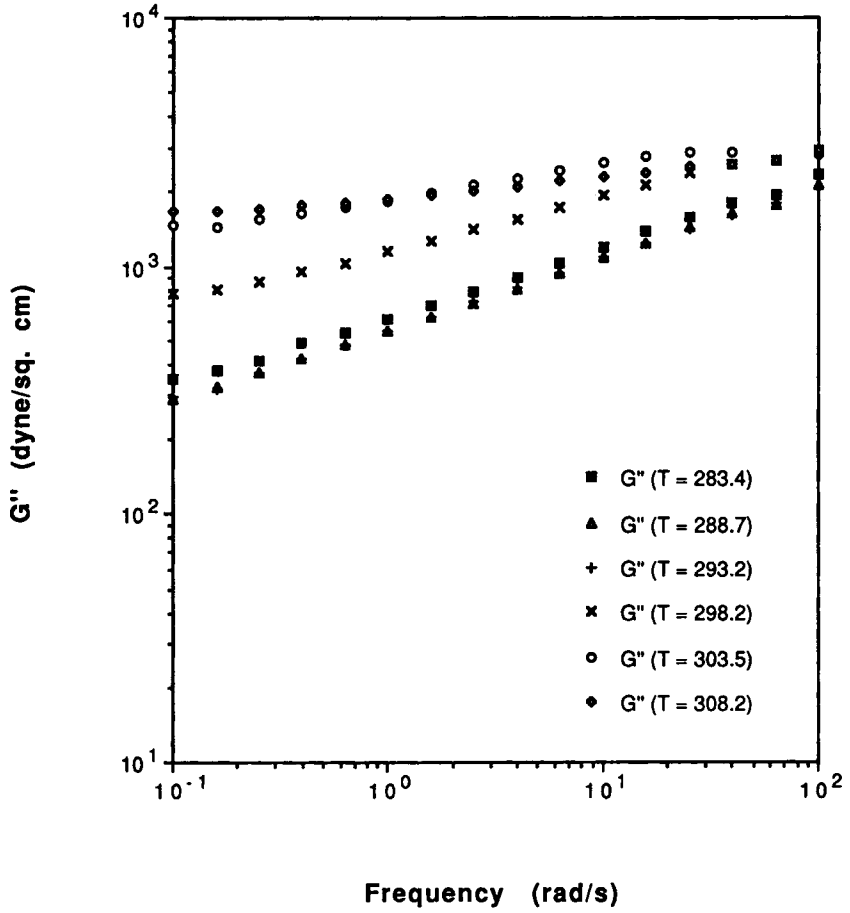

Figure 2 Dynamic rheological measurements in the linear viscoelastic region for G'' vs. frequency. Measurement conditions are described in the text.

$$H(t) = [(2/\pi)3^{n''/2}a''(1 - n'')]t^{-n''} \quad (6)$$

Values of K' $\{=[a'n'\ (1 - n'/2)2^{n'/2}]\}$ and K'' $\{= [(2/\pi)3^{n''/2}a''(1 - n'')]\}$ are tabulated in Table III and show that the two approximations agree within about 25%. It should be noted from Table III that $H(t)$ declines with increasing t for all dispersions but the rate of decline is a function of tem-

Table I Effect of Temperature on Linear Viscoelastic Behavior of Storage Modulus for Collagen Dispersions

Temperature	a'	n'	r^2
283.3	1,484.0	0.265	0.999
288.7	1,140.7	0.298	0.998
293.2	1,177.8	0.290	1.000
298.2	5,679.7	0.149	0.998
303.5	11,647.0	0.108	0.999
308.2	11,428.0	0.063	0.994

Parameters a' and n' were computed from a linear-least squares analysis of the data in Figure 1 applied to eq. (1): $G' = a'\omega^{n'}$. r is the correlation coefficient from the linear-least-squares analysis. The units of temperature are Kelvin; of G', dyne/sq cm; and of ω, rad/s.

Table II Effect of Temperature on Linear Viscoelastic Behavior of Loss Modulus for Collagen Dispersions

Temperature	a''	n''	r^2
283.3	620.9	0.284	0.999
288.7	552.0	0.291	0.999
293.2	552.6	0.288	1.000
298.2	1178.7	0.204	0.996
303.5	1870.4	0.113	0.951
308.2	1911.6	0.081	0.981

Parameters a'' and n'' were computed from a linear-least-squares analysis of the data in Figure 2 applied to eq. (2): $G'' = a''\omega^{n''}$. r is the correlation coefficient from the linear-least-squares analysis. The units of temperature are Kelvin; of G'', dyne/sq cm; and of ω, rad/s.

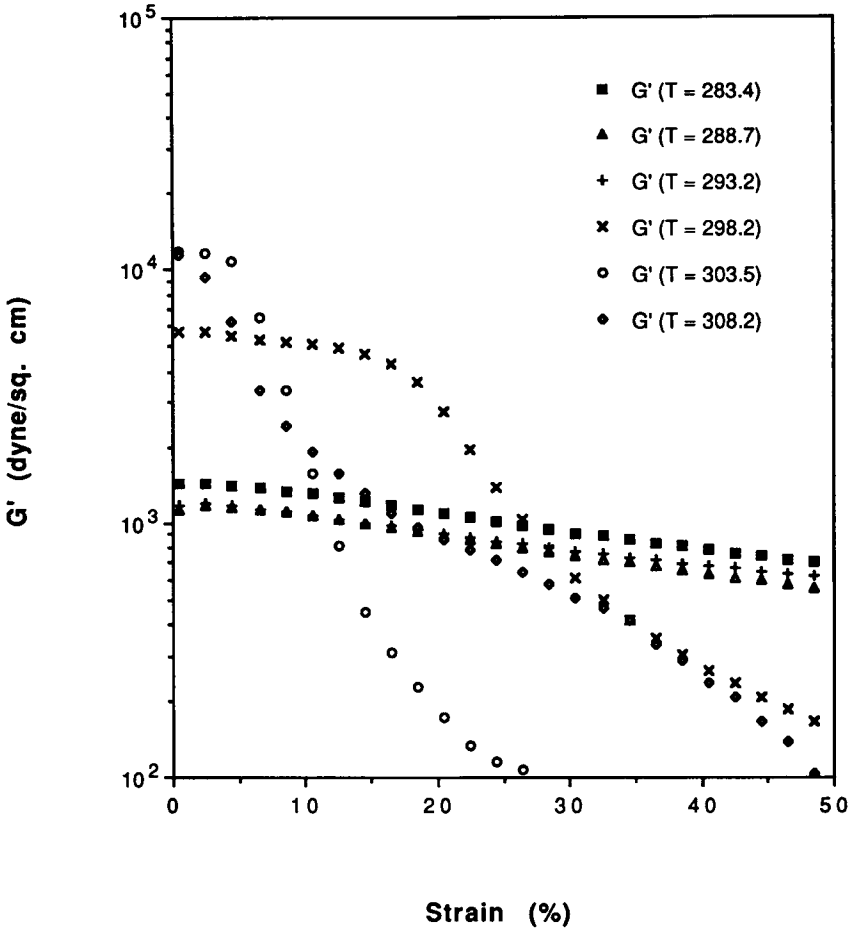

Figure 3 Measurements of G' vs. strain (at 1 rad/s) for dispersions of varying temperature. Measurement conditions are described in the text.

perature. Ferry[20] discussed the significance of the slope of $H(t)$ and showed that fluidlike viscoelastic materials have a steeper decline in $H(t)$ vs. t (larger n' or n'') than have more rigid viscoelastic materials.

DISCUSSION

Relationship between Rheological Spectra and Collagen Fiber Mechanical Properties

The materials studied here are a dispersion of collagen fibers in a physiologic buffer. A relationship between the average rigidity of individual fibers and the measured rheology of the entire dispersion is developed from the theory of Kamphuis and Jongschaap.[21,22] The reported increase in collagen fiber formation kinetics[4-6,14] with increasing temperature has been attributed to an increase in intermolecular attractive forces with increasing temperature. Increases in intermolecular attractive forces would also be expected to increase the molecular ordering in fibers. Mechanically, this increase in intermolecular attractive forces would plausibly be expected to translate into enhanced fiber rigidity. Recent photomicrographs show that increasing intermolecular attractive forces in collagen fibers by decreasing ionic strength increases fiber rigidity through an increase in the packing density and molecular ordering in fibers.[23]

A mechanistic and quantitative interpretation of the dependence on the slope of the relaxation-time spectrum on fiber rigidity may be obtained by considering the model of Kamphuis and Jongschaap[21,22] for concentrated dispersions. Their model describes the mechanical properties of a network of interconnected webs (or chains) with solvent trapped between the web junctions (points where chains intersect). For collagen fiber dispersions, each fiber would correspond to one chain. As derived in Ref.

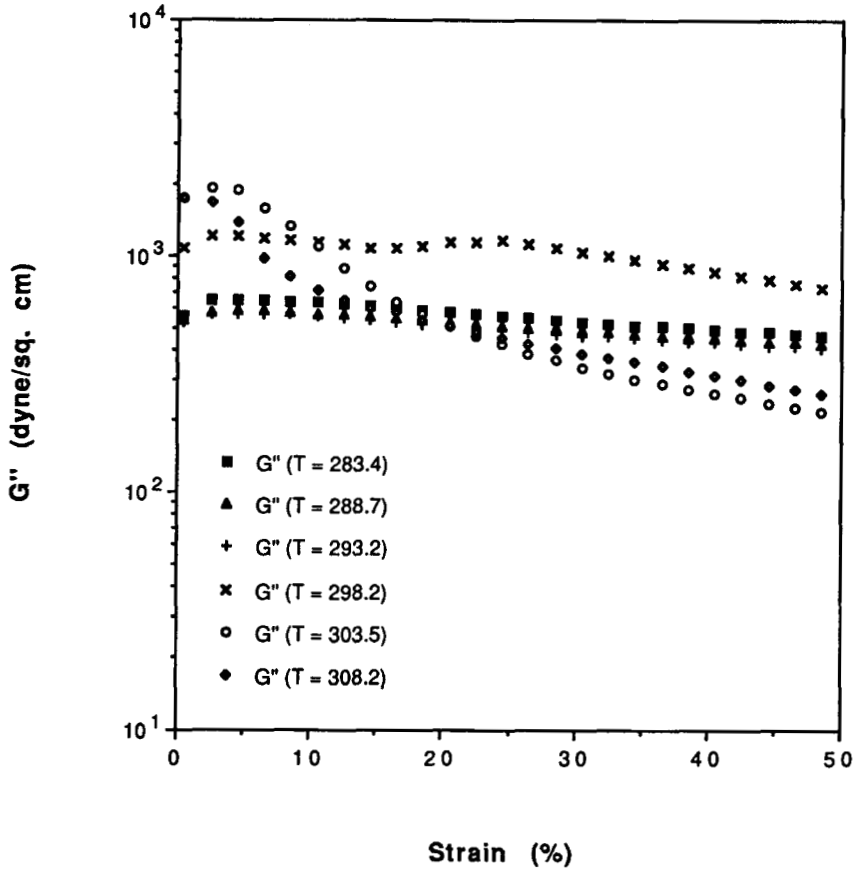

Figure 4 Measurements of G'' vs. strain (at 1 rad/s) for dispersions of varying temperature. Measurement conditions are described in the text.

21, the rheology is described by a statistical mechanics transient network model where the chains are idealized as linear springs. The model allows for nonaffine deformation of chains by assuming that chains deform and chain junctions rupture so as to equally distribute forces throughout the network. Chain junction formation and rupture is described by a structure kinetics equation and the anisotropic contribution to the stress tensor is computed by averaging the dyad of the chain-length vector and chain-force vector over the distribution of chain lengths and orientations. Kamphuis et al. gave the following expressions for the relaxation time (t_i) and modulus (G_i) for the ith relaxation mode in a system of similar-type chains:

$$t_i = 1/(ih_0) \tag{7}$$

$$G_i = \begin{cases} n_0 q_0/15\{3f_0 + (1 + f_0/c)[c/(1 + \lambda)]\} & i = 1 \\ n_0 q_0/15\{(1 + f_0/c)[c/(1 + \lambda c)] \times [\lambda c/(1 + \lambda c)]^{i-1}\} & i > 1 \end{cases} \tag{8}$$

where h_0 is the rate constant for chain rupture; n_0, the initial chain number density; q_0, the initial av-

Table III Temperature Dependence of Linear-Viscoelastic-Time-Spectrum Coefficients K' and K'' as Defined in the Text

Temperature	K'	K''
283.3	374.0	330.8
288.7	320.8	292.3
293.2	322.9	293.4
298.2	824.7	670.0
303.5	1235.3	1123.8
308.2	712.9	1168.6

The coefficients K' and K'' are defined in the text and have units of dyne/sq cm. The exponents n' and n'' corresponding to $H(t)$ in eqs. (5) and (6) are tabulated in Tables I and II, respectively.

erage chain-length vector; f_0, the average initial force per chain; c, the chain spring constant; and λ, a parameter that describes the degree to which the deformation is nonaffine. The rigidity of the fibers is reflected in c, the fiber elasticity constant. For nonaffine flow, which most likely occurs in the concentrated dispersions studied here, the long time-relaxation modes [smaller i—from (7)] proportionately weight network configuration (n_0, q_0) as well as chain elasticity (c). Shorter time modes (larger i) display an increasing importance of the chain elasticity (on G_i) as the $[\lambda c/(1 + \lambda c)]$ term in $(8 - i > 1)$ is raised to the $i - 1$ power. This is particularly important for very short time modes. In contrast, the effect of network configuration (n_0, q_0) on G_i is linear for all relaxation time modes.

The relationship between G_i and $H(t)$ can be seen from a comparison of the dependence of $G'(\omega)$ on both terms[20]:

$$G'(\omega) = \sum_i \{G_i \omega_i^2 t_i^2/(1 + \omega_i^2 t_i^2)\} \quad (9a)$$

$$G'(\omega) = \int \{H(t)\omega_i^2 t_i^2/(1 + \omega_i^2 t_i^2)\} d \ln t \quad (9b)$$

Equations 9(a) and 9(b) show that both G_i and $H(t)$ reflect the magnitude of specific time-dependent relaxation modes and that they differ only in that $H(t)$ is a continuous representation of this functional dependence and G_i is a discrete representation. For a rigid solid [where $G'(\omega)$ would be constant], the only nonzero G_i occurs when t_i becomes infinite [eq. (9a)]. The rigid solid corresponds to the case [from eq. (1)] where n' goes to zero. Consequently, for the dispersions with smaller values of n', only the long t_i relaxation mechanisms are significant, whereas for dispersions with larger values of n', shorter t_i relaxation mechanisms gain increasing significance. Rigid fibers correspond to c [in eq. (8)], becoming very large. In this limit, the $i = 1$ (longest-time mode) value of G_i will be much greater than values of G_i for $i > 1$ (shorter-time modes). Therefore, rigid fiber dispersions correspond to the rheological spectra where n' is small since both limits (n' small, c large) require the longest time-relaxation modes to dominate. Conversely, flexible fiber dispersions correspond to spectra with larger values of n'. In a dispersion, shorter time-relaxation modes correspond to fast intrafiber relaxation (elastic fiber contractions) and longer time-relaxation modes correspond to slower interfiber relaxation (fibers in unfavorable entanglement configurations rearrange to more favorable configurations). This interpretation is based on the fact that shorter time-relaxation modes are much more strongly weighted by chain elasticity [in eq. (8)], whereas longer-time modes more proportionately weight chain configuration. The effect of increasing temperature in collagen fiber dispersions is a progressive rigidification of the fibers, as can be seen from the data (measured values of n') in Figure 1.

Relationship between Mechanical Properties of a Collagen Fiber and Molecular Packing

The effect of packing of collagen molecules on the rigidity of a collagen fiber can be further described by considering theories describing the rheology of rigid-rod polymer liquid crystalline phases (LCPs). The analogy here is that the collagen fiber is a very concentrated LCP of rodlike collagen molecules. Matheson[24] developed a theory for the viscosity (η) of an LCP of monodisperse rigid-rod polymers where η is related to an order parameter (y), the rod volume fraction in the LCP (ϕ), and the maximum possible rod volume fraction at tight packing (ϕ_{max}) as

$$\eta \sim y^2\{\phi/(1 - \phi/\phi_{max})\}. \quad (10)$$

The order parameter, y, is a function of the degree of rod alignment in the LCP. The theory predicts that at small rod volume fractions ($\phi < 0.3$) increased rod alignment in the LCP reduces the LCP viscosity; however, at $\phi > 0.3$, η begins to dramatically increase with increasing ϕ. The effect of the rod volume fraction becomes especially pronounced as ϕ approaches ϕ_{max}. Applying these concepts to collagen fibers suggests that they become more rigid as η increases. The rigidification of collagen fibers is expected to correspond to collagen molecule packing conditions where ϕ approaches ϕ_{max}. The Matheson theory predicts that in a concentrated LCP (such as a collagen fiber) the mechanical response will be dominated by the volume fraction of solvent remaining in the LCP.

One complexity not considered in the Matheson theory is that the collagen fibers studied here contain a polydisperse rod (molecule) size distribution.[25] Aharoni[26] developed a theory for η in LCPs composed of polydisperse rigid rods. The Aharoni theory predicts behavior similar to the Matheson theory where at $\phi > 0.4$, η increases precipitously with increasing ϕ due to close-packing effects. Thus, it is clear that the measured changes in collagen fiber rigidity as temperature increases must be accompanied by a decrease in the water volume fraction in the fibers.

Relationship between Temperature and Molecular Packing in Collagen Fibers

Insight into the mechanism by which temperature alters the volume fraction of solvent in collagen fibers can be obtained by considering the extended Flory–Matheson theory[27] for the effect of thermal contributions to the phase equilibrium of collagen fibers. The extended Flory–Matheson theory applies the more general Flory theory[28] for the equilibrium of phase-separated rigid-rod polymers to collagen. The Flory theory predicts the volume fraction of solvent and rod-polymer in both the separated LCP as well as in the nonseparated solvent phase. The phase equilibrium predictions depend on the magnitude of the Flory χ parameter, which describes the interaction energies between solvent molecules and rod-polymer molecules. The thermal dependence of χ can be calculated from the thermal dependence of the free energies of bonding for hydrophobic side chains along adjacent collagen triple helices. Wallace[29] gave a form for the temperature dependence of χ that is derived by summing temperature-dependent contributions over the 36 aromatic and 188 aliphatic amino acid side chains on the collagen triple helix that are capable of participating in hydrophobic bonding. The resulting χ is a monotonically increasing function of temperature over the temperature range studied here:

$$\chi = -b\{[1790 - 11.8T + 0.0162T^2]/[RT]\} \quad (11)$$

where T is temperature (in Kelvin); R, the universal gas constant (in calories); and b, a fitting parameter.

The extended Flory–Matheson theories permit a description of the thermal dependence of molecular events associated with fiber rigidification. The theory predicts phase diagrams where the volume fraction of rods (collagen molecules) in the anisotropic (fiber) phase is strongly dependent on χ. For rods with large aspect (length/diameter) ratios such as collagen, the phase diagram shifts rapidly to increased collagen volume fractions in fibers (i.e., rigidification) over a narrow range of χ once χ exceeds 0.09. The thermally induced changes seen in Figures 1–4 appear to be a consequence of passage through this transition range.

Calculations of the volume fraction of solvent present in collagen fibers as a function of temperature were performed for comparison with the measured rheological properties of the fiber dispersions. Since the collagen used in these experiments was pepsin-digested, a variation of the Flory equilibrium theory was employed[27] that could account for the presence of the residual portion of the C-terminal telopeptide of collagen that is not cleaved during enzyme digestion. Details of the phase equilibria calculations have been described elsewhere.[29] Computations of the solvent and rod volume fractions in collagen fibers corresponding to the range of conditions studied experimentally are presented in Table IV. The results show that based on thermodynamic principles the variation in the solvent volume fraction in the collagen fibers is small; however, since collagen volume fractions in fibers are nearly at ϕ_{max}, the changes in Table IV correspond [in eq. (10)] to a range where η (hence, rigidity) of the fibers changes precipitously. There are several practical complications in this system that might make the actual water volume fractions in collagen fibers different from those calculated in Table IV. The theoretical calculations were premised on a system composition of monodisperse rods that are linear. The collagen employed in these studies is known to have significant polydispersity,[25] containing both rods that are double or triple the length of a collagen monomer (oligomers) as well as rod fragments that are shorter in length than a collagen monomer.[30] In addition, it is possible for higher-order oligomers to be branched.[25] In polydisperse rod systems, LCPs are known to grow by incorporating the largest length rods first.[26,31] Thus, with fiber nuclei containing a high concentration of collagen oligomers, it is unlikely that collagen fibers could grow with packings as dense as the theoretical predictions would suggest. This effect is further exacerbated by

Table IV Phase Equilibrium Calculations of Collagen Volume Fractions in Both Fiber and Solvent Phases in Collagen Fiber Dispersions

T	Δf_{el}	Δf_h	ϕ	ϕ'
280	−5.33	−60.0	9.51×10^{-4}	0.914
289	−5.42	−65.7	2.19×10^{-4}	0.921
304	−5.57	−73.8	5.51×10^{-5}	0.926
309	−5.62	−76.0	4.02×10^{-5}	0.927

Calculations are based on an initial dispersion of monodisperse pepsin-digested collagen monomers. Collagen fiber dispersions are at pH 7.2 and ionic strength = 0.20. T is the temperature of the dispersion. Δf_{el} and Δf_h are the free energies (in calories) per mol of polymer segments employed in computing the Flory χ-factor in the phase equilibria calculations (there are 201 polymer segments in a pepsin-digested collagen monomer). Calculation of these terms is described in detail in Refs. 16 and 27. ϕ is the volume fraction of soluble collagen in the solvent (water) phase and ϕ' is the volume fraction of collagen in the (phase-separated) fiber phase.

the presence of branched oligomers. Finally, there is evidence[32] that even small defects in collagen molecules significantly impact the structure of fibers that grow. In these studies, point mutations of amino acids in collagen monomers yielded fibers substantially less robust than fibers grown from nondefective monomers.

Complications in Interpreting Collagen Fiber Properties from Theories of Molecular Packing

An additional factor that complicates the interpretation of experimental behavior in terms of thermodynamic models is that the experiments were performed on fibers that were precipitated at 290 K, stored at 277 K for an extended period of time, and then incubated at the measurement temperature for a short period prior to recording the rheological spectrum (samples were stored at the colder temperature to retard bacterial growth and intermolecular cross-linking). In contrast, the model predictions were based on soluble collagen molecules phase-separating into fibers. The process is not completely reversible because collagen molecules undergo cross-linking[33] when in the fibrillar state. Partial cross-linking (which increases with incubation time at elevated temperatures) would have a similar effect on oligomers in altering the equilibrium rod volume fractions that would be attained in collagen fibers. The measured rheological properties might also reflect only partial fiber reassembly (at measurement temperatures) in dispersions that were thermally disassembled (at the storage temperature). Reassembly of fibers to equilibrium volume fractions in such a highly concentrated system could proceed *very* slowly. It is also possible that a different type of equilibrium is occurring here, namely, one in which fibers disassemble into microfibrils that can reaggregate (altering the water content of the fibers) while the microfibrils (which are what the Flory theory describes) retain a fairly constant water volume fraction. The assembly of collagen fibers through this pathway has recently been considered.[34] Even though incubation times at measurement temperatures were determined from the interval required for the rheological spectra to become invariant, it is possible that measurements were performed on dispersions that were not at equilibrium, but were kinetically trapped in a nonequilibrium state. Precipitating the fibers at specific temperatures and incubating the dispersions at those temperatures might therefore yield different results.

There is an effect of viscosity change in the solvent over the temperature range studied. Increased solvent viscosity would tend to enhance fiber rigidity in the anisotropic (fiber) phase without necessarily any changes in molecular ordering. This effect is due to increased frictional resistance to the relative motion of neighboring molecules in fibers (which is how fibers deform). It is most likely the reason for the increased fiber rigidity at 283 K relative to 288 K (see Figs. 1 and 2). Decreases in solvent viscosity would likely contribute to enhanced flexibility in the absence of changes in intermolecular attractive forces. It is therefore possible that incipient fiber rigidification is occurring between 283 and 288 K, but its effect is obscured by the decrease in solvent viscosity over this temperature range. The viscosity of water decreases from 0.00131 to 0.00114 Pa-s (Ref. 35) between 283 and 288 K and the linear viscoelastic spectra (Figs. 1 and 2) change in similar proportion. Based on theories for the dynamics of rodlike molecules,[36] a linear dependence on solvent viscosity would be expected. Between 288 and 293 K, the viscosity of water decreases from 0.0014 to 0.0010 Pa-s,[35] yet the linearly viscoelastic rheological spectra are nearly identical. It is likely that weak incipient hydrophobic attractive forces offset the decrease in solvent viscosity over this temperature range and only at temperatures above 293 K do hydrophobic forces become dominant in the system.

Nonlinear Dynamic Rheological Behavior

Onogi and Matsumoto[37] and Komatsu et al.[38] experimentally studied the nonlinear rheological behavior of emulsions and suspensions. They report master plots of the frequency response of G' and G'' over a wide range of strain amplitudes for concentrated suspensions of a styrene copolymer in polystyrene solution. At frequencies of less than 0.1 s^{-1} (approximately 0.6 rad/s), there is minimal strain thinning, whereas at frequencies greater than 0.6 rad/s, strain thinning becomes more pronounced. G' decreases by an order of magnitude or more at the higher frequencies. Similar nonlinear spectra for oil-in-water emulsion-like creams were measured at various strain amplitudes (but at lower strains than the suspensions discussed previously). These emulsions display maximum strain thinning at frequencies of approximately 0.06 rad/s with less strain thinning at higher frequencies. Thus, frequencies above 0.6 s^{-1} are sensitive to differences between suspension- and emulsionlike particle behaviors in

dispersions (even when the suspension is in a polymer solvent). Figures 3 and 4 show significant differences in the strain thinning behavior of collagen dispersions as a function of temperature (measured at 1 rad/s). Dispersions at low temperatures (more flexible fibers) display less strain thinning than do high-temperature (more rigid fibers) dispersions. Thus, the dispersion appears to undergo a transition from emulsion-like to suspension-like behavior as temperature increases.

This behavior is consistent with the results of the linear viscoelastic measurements where lower temperatures result in weaker fiber-intermolecular attractive forces, more flexible fibers, and a more emulsion-like dispersion. Dispersions at higher temperatures, in contrast, are subject to greater intermolecular attractive forces that give more rigid fibers and result in a more suspension-like dispersion. The jump in the low-strain value of G' at temperatures greater than 293 K is probably a result of the formation of a gel (3-dimensional fiber network) due to the presence of sufficient fiber rigidity and sufficiently strong interfiber attractive forces. Similar gel-like behavior has been reported for other rigid rod polymers that phase-separate into LCPs.[39]

CONCLUSIONS

Hydrophobic forces in collagen fiber dispersions mediate the dispersion rheological behavior through changes in fiber rigidities. These forces act in phase-separated collagen fibers when amino acid side chains on adjacent molecules can juxtapose in close enough proximity to hydrophobically bond. These forces increase strongly with temperature over the ranges of temperature studied here. Fiber rigidities appear to be altered by changes in the water volume fraction in the fibers. Gelation of phase-separated rod-molecule hydrogels such as collagen proceeds by rigidification of the phase-separated fibers. Polydispersity, other defects in the collagen monomers, and nonequilibrium conditions can significantly impact the fiber structure and, consequently, the range of temperatures over which fiber rigidities change. From a practical standpoint, the gelation of concentrated collagen dispersions above 298 K allows this material to be easily injected when refrigerated yet form a stiffer gel at physiologic temperatures. Its widespread use as a structural filling agent in soft tissue augmentation[40] applications would not be effective without this change in the material.

REFERENCES

1. T. R. Knapp, E. N. Kaplan, and J. R. Daniels, *Plast. Reconst. Surg.*, **60,** 39 (1977).
2. S. T. Stegman and T. A. Tromovitch, *J. Dermatol. Surg. Oncol.*, **6,** 450 (1980).
3. D. G. Wallace and A. Thompson, *Biopolymers,* **25,** 1793 (1983).
4. R. A. Gelman, B. R. Williams, and K. A. Piez, *J. Biol. Chem.*, **254,** 180 (1979).
5. B. R. Williams, R. A. Gelman, P. C. Poppke, and K. A. Piez, *J. Biol. Chem.*, **253,** 6578 (1978).
6. A. Veis and K. Payne, in *Collagen Vol. I,* M. Nimni, Ed., CRC Press, Boca Raton, FL, 1988, pp. 114–137.
7. D. G. Wallace, W. Rhee, and B. Weiss, *J. Biomed. Mater. Res.*, **21,** 861 (1987).
8. D. G. Wallace, W. Rhee, H. Reihanian, G. Ksander, R. K. Lee, W. B. Braun, B. A. Weiss, and B. B. Phar-riss. *J. Biomed. Mater. Res.*, **23,** 931 (1989).
9. J. Woodhead-Galloway, in *Collagen in Health and Disease,* J. B. Weiss and M. I. Jayson, Eds., Longman Group Ltd., Edinburgh, 1982, Chap. 3.
10. G. C. Na, L. J. Phillips, and E. I. Freire, *Biochemistry* **28,** 7153 (1989).
11. J. W. Smith, *Nature,* **219,** 157 (1968).
12. R. D. B. Fraser, T. P. McRae, and A. Miller, *J. Mol. Biol.*, **193,** 115 (1987).
13. Y. Bouligand, J.-P. Denefle, J.-P. Lechaire, and M. Maillard. *Biol. Cell,* **54,** 143 (1985).
14. H. B. Bensusan and B. L. Hoyt, *J. Am. Chem. Soc.*, **80,** 717 (1957).
15. J. A. Chapman, D. F. Holmes, K. M. Meek, and C. J. Rattew, in *Structural Aspects of Recognition and Assembly in Biological Molecules,* M. Balaban, Ed., Intl. Sci. Services, Rehovot/Philadelphia, 1981, pp. 387–401.
16. D. G. Wallace, *Biopolymers,* **29,** 1015 (1990).
17. M. J. Capaldi and J. A. Chapman, *Biopolymers,* **21,** 2291 (1982).
18. D. G. Wallace, R. A. Condell, J. W. Donovan, A. Paivinen, W. M. Rhee, and S. B. Wade, *Biopolymers,* **25,** 1875 (1986).
19. J. C. Scanlon and H. H. Winter, *Macromolecules,* **24,** 47 (1991).
20. J. D. Ferry, *Viscoelastic Properties of Polymers,* 3rd ed., Wiley, New York, 1980, Chaps. 3, 4.
21. H. Kamphuis, R. J. J. Jongschaap, and P. F. Mijnlieff, *Rheol. Acta,* **23,** 329 (1984).
22. H. Kamphuis and R. J. J. Jongschaap, *J. Rheol.*, **29**(6), 685 (1985).
23. J. Rosenblatt, B. Devereux, and D. Wallace, *Biomaterials,* **13,** 878 (1992).
24. R. R. Matheson, *Macromolecules,* **13,** 643 (1980).
25. A. W. Chow, G. G. Fuller, D. G. Wallace, and J. A. Madri, *Macromolecules,* **18,** 793 (1985).
26. S. M. Aharoni, *Polymer,* **21,** 1413 (1980).
27. R. R. Matheson and P. J. Flory, *Macromolecules,* **14,** 954 (1981).

28. P. J. Flory, *Proc. R. Soc. Lond. Ser. A,* **234,** 73 (1956).
29. D. G. Wallace, *Biopolymers,* **30,** 889 (1990).
30. A. W. Chow, G. G. Fuller, D. G. Wallace, and J. A. Madri, *Macromolecules,* **18,** 805 (1985).
31. J. K. Moscicki and G. Williams, *Polymer,* **24,** 85 (1983).
32. D. J. Prockop, *J. Biol. Chem.,* **256**(26), 15349 (1990).
33. M. Yamanuchi and G. Mechanic, in *Collagen Vol. I, Biochemistry,* M. Nimni, Ed., CRC Press, Boca Raton, FL, 1983, Chap. 6.
34. D. Wallace, *Biopolymers,* **32,** 497 (1992).
35. R. C. Weast and M. J. Astle, Eds., *Handbook of Chemistry and Physics, 63rd ed.,* CRC Press, Boca Raton, FL, 1983, p. F-40.
36. M. Doi and S. F. Edwards, *The Theory of Polymer Dynamics,* Clarendon Press, Oxford, 1986, Chaps. 8–10.
37. S. Onogi and T. Matsumoto, *Polym. Eng. Rev.,* **1,** 45 (1981).
38. H. Komatsu, T. Mitsui, and S. Onogi, *Transact. Soc. Rheol.,* **17**(2), 351 (1973).
39. S. Z. D. Cheng, S. K. Lee, J. S. Barley, S. L. C. Hsu, and F. W. Harris, *Macromolecules,* **24,** 1883 (1991).
40. J. M. Pachence, R. A. Berg, and F. H. Silver, *Med. Dev. Diag. In.* **Jan,** 49 (1987).

Received October 20, 1992
Accepted March 14, 1993